Environmental Engineering and Management Journal

October 2014, Vol.13, No. 10, 2551-2559
http://omicron.ch.tuiasi.ro/EEMJ/

"Gheorghe Asachi" Technical University of Iasi, Romania

EQUILIBRIUM, KINETIC AND THERMODYNAMIC STUDIES OF CATIONIC RED X-GRL ADSORPTION ON GRAPHENE OXIDE

Jiankun Sun[1], Yanhui Li[1*], Tonghao Liu[1], Qiuju Du[1], Yanzhi Xia[1], Linhua Xia[1], Zonghua Wang[1], Kunlin Wang[2], Hongwei Zhu[2], Dehai Wu[2]

[1]*Qingdao University, College of Electromechanical Engineering, Laboratory of Fiber Materials and Modern Textile, the Growing Base for State Key Laboratory, 308 Ningxia Road, 266071 Qingdao, China*
[2]*Tsinghua University, Key Laboratory for Advanced Manufacturing by Material Processing Technology and Department of Mechanical Engineering, 100084 Beijing, China*

Abstract

Graphene oxide (GO) was prepared from expandable graphite by a modified Hummers' method and characterized by TEM, XRD, FTIR, and Raman spectroscopy. The batch adsorption experiments were carried out to study the effect of various parameters, such as the initial concentration, adsorbent dosage, initial pH, contact time and temperature on adsorption properties of cationic red X-GRL onto GO. The Langmuir and Freundlich models were used to fit the experimental data of adsorption isotherms. The kinetic studies showed that the adsorption data followed the pseudo-second order model. Thermodynamic studies indicated the reaction of cationic red X-GRL adsorbed by GO was a spontaneous and endothermic process. The results indicated that GO could be considered a promising adsorbent for the removal of dyes from aqueous solutions.

Key words: adsorption, cationic red X-GRL, graphene oxide (GO), kinetics, thermodynamics

Received: September, 2011; Revised final: June, 2012; Accepted: June, 2012

1. Introduction

Various types of dyes, more than 100, 000 types commercially available, are indispensable to the textile, rubber, plastics, paper and leather industries (Robinson et al., 2001). Many of them are toxic and non-biodegradable in nature and stable to light and oxidation. Effluents containing dyes beyond permissible concentration can reduce light penetration and photosynthesis (Sun and Yang, 2003) and cause irreparable damage to human being as well as aquatic and terrestrial living beings. Common methods for the treatment of dye effluents include adsorption (Harja et al., 2011), electrocoagulation (SenthilKumar et al., 2010), oxidation (Malik et al., 2003), flocculation (Panswed et al., 1986), ozonation process (Koch et al., 2002), membrane separation (Ciardelli et al., 2000), and micellar enhanced ultrafiltration (Purkait et al., 2003). Adsorption is growing in popularity due to its advantages of simple operation, low cost, rapid treatment and effectiveness for removing low dye concentration waste streams. Various adsorbents such as clay, perlite, zeolite, and unburned carbon (Alpat et al., 2008) have been developed and used to remove dyes from aqueous solution. However, increasingly stringent standard on the quality of drinking water has stimulated a growing effort on the exploiture of new high effcient adsorbents.

Recently, graphene is receiving increased attention due its unique structure, unusual physical and mechanical properties such as high carrier concentration and mobility (Morozov et al., 2005), high thermal conductivity (Balandin et al., 2008), and high mechanical strength (Lee et al., 2008). Similar to graphene, GO also has a layered structure and it

* Author to whom all correspondence should be addressed: e-mail: liyanhui@tsinghua.org.cn; xiayzh@qdu.edu.cn; Fax: +86 532 85951842

can be obtained in high yield by controlled chemical oxidation of graphite (Park, and Ruoff, 2009). GO can be easily functionalized with phenolic, carboxyl, epoxide and other groups by oxidation treatment (Zhang et al., 2010a).

There have been some studies about using GO as an adsorbent to remove heavy metals and methylene blue from contaminated drinking water (Yang et al., 2010, 2011). In addition, some composites, such as GO /MnO_2, GO/Ag (Sreeprasad et al., 2011), GO/ferric hydroxide (Zhang et al., 2010b), were also developed as adsorbents in water purification and showed exceptional adsorption properties for Hg (II) and arsenate in aqueous solutions.

However, to our knowledge, few investigations have been carried on the use of GO as an adsorbent for dyes removal. In this work, GO was prepared and characterized by TEM, XRD, FTIR, and Raman spectroscopy. The effect of various experimental parameters on cationic red X-GRL adsorption process, such as pH, initial dye concentration, contact time, and temperature were studied. Equilibrium isotherm, kinetic and thermodynamic studies of dye adsorption on GO have been studied and analyzed.

2. Material and methods

2.1. Materials

The expandable graphite was purchased from Qingdao Henglide Graphite Co. Ltd., China. Potassium permanganate, 98% sulfuric acid, sodium nitrate, hydrochloric acid and 30% hydrogen peroxide were of analytical grade and purchased from Sinopharm Chemical Reagent Co. Ltd., China. The cationic red X-GRL (AR grade) was obtained from Shanghai Reagents Co. Ltd., China.

2.2. Preparation of GO

GO was synthesized from expandable graphite by following a modified Hummers' method (Hummers and Offeman, 1958) reported previously from our group (Liu et al., 2012). In brief, 5.0 g of expandable graphite was dispersed into a mixture of concentrated sulfuric acid (230 mL), sodium nitrate (5.0 g) and potassium permanganate (30 g) at 273 K. After the mixture was stored in refrigerator at 273 K for 24 h, it was stirred at 308 K for 30 min and diluted with deionized water to 690 mL. Then, the reaction temperature of the suspension was rapidly increased to 371 K in an oil bath and maintained for 30 min.

Finally, 1400 mL distilled water and 100 mL of 30% H_2O_2 solution were added after the reaction. The mixture was washed with 5% HCl and distilled water several times. After filtration and drying at 283 K, GO was obtained.

2.3. Characterization of GO

The morphology and microstructure of the sample were characterized by a Transmission electron microscope (TEM, JEM-2100F, operated at 200 kV), X-ray diffraction(XRD, Bruker D8 diffractometer with Cu Kα radiation, λ =1.5418 Å, a scan rate of 0.02°2θ/s from 5 to 70°) , Raman microscope (Renishaw RM2000 Raman microscope) and Fourier transformation infrared spectra (FTIR, Perkin-Elmer-283B FTIR spectrometer, the wave number range from 400 to 4000 cm^{-1}).

2.4. Batch adsorption experiments

A stock solution of cationic red X-GRL (1000 mg L^{-1}) was prepared by dissolving appropriate amounts of cationic red X-GRL in deionized water. The stock solution was diluted to required concentrations before used. The batch adsorption experiments were carried out by using the GO as the adsorbent. 100 mL solution of known X-GRL concentration and a certain amount of GO were added into 250 mL conical flasks and then shook in a temperature-controlled water bath shaker (SHZ-82A). The initial pH of GO solution is about 4, so it is used in the further studies.

The concentration of cationic red X-GRL was measured by ultraviolet spectrophotometer (TU-1810, Beijing Purkinje General Instrument Co., Ltd, China).The absorbance is $max_{X\text{-}GRL}$=532 nm for cationic red X-GRL. The adsorption capacity, i.e. amount of cationic red X-GRL adsorbed by GO at equilibrium, was evaluated using the following Eq. (1):

$$q_e = (\frac{C_0 - C_e}{m})V \quad (1)$$

where q_e is the GO adsorption capacity (mg g^{-1}), C_0 and C_e are initial and equilibrium concentration of cationic red X-GRL (mg L^{-1}) in solution, m is the mass of adsorbent (g), V is volume of the solution (L).

The dye removal percentage Q (%) at time t is calculated by the following Eq. (2):

$$Q = \frac{C_0 - C_t}{C_0} \times 100\% \quad (2)$$

where C_0 (mg L^{-1}) is the initial concentration of cationic red X-GRL, C_t (mg L^{-1}) is the concentration of cationic red X-GRL at time t.

The effect of pH on cationic red X-GRL removal was studied by adding 0.03 g GO into 100 mL of the solution with dye concentration of 50 mg L^{-1} and adjusting initial pH ranging from 2.0 to 10.5 at 293 K and agitating for 1.5 h. The pH of the solution was adjusted with negligible amount of different concentrations of HNO_3 (0.1, 0.05, 0.01 mol L^{-1}) or NaOH (0.1, 0.05, 0.01 mol L^{-1}) solution.

The effect of adsorbent dosage on cationic red X-GRL removal was conducted by shaking 100 mL of 100 mg L^{-1} dye solution containing different GO dosage at 293 K. The range of the GO dosage was from 0.03 to 0.13 g in a step size of 0.02 g.

A series of contact time experiments for cationic red X-GRL were carried out at the pH of solution (pH=4) and temperature of 293 K. 0.6 g GO was added into 2000 mL solution with different cationic red X-GRL concentrations of 20 and 40 mg L^{-1}. At the predetermined time, the samples were collected by using a 0.45 μm membrane filter and analyzed. To evaluate the thermodynamic properties, 0.03 g GO was added into 100 mL solution with initial cationic red X-GRL concentrations ranging from 20 to 70 mg L^{-1}. The pH of solution was adjusted to 4. These samples were then shaken continuously for 1.5 h at 293, 313, 333 K, respectively.

3. Results and discussion

3.1. Characterization of GO

Fig. 1a shows a typical TEM image of GO prepared by the modified Hummers' method. It can be seen that most GO are of single to a few layers thick and stacked together.

The Raman spectrum of GO is very sensitive to the number of atomic layers and the presence of disorder or defects on carbonaceous materials and it has proved to be an essential tool to characterize graphite and graphene materials (Calizoa et al., 2009). Raman spectrum of GO (Fig. 1b) shows a D band peak at 1363 cm^{-1} that corresponds to the breathing mode of κ-point phonons of A_{1g} symmetry. The D band is associated with vibrations of carbon atoms with dangling bonds in plane terminations of disordered graphite and appears as a strong band when the number of GO oxide layers in a sample is large (Rao et al., 2009). The G band peak at 1583 cm^{-1} corresponds to an E_{2g} mode of graphite and is related to the vibration of sp2-bonded carbon atoms (Rao et al., 2009; Shen et al., 2009). The second-order 2D band is observed at 2688 cm^{-1}. The strong 2D band peak suggests that the synthesized GO has considerable defects (Cuong et al., 2010).

The diffraction peak at 10.69º in the XRD pattern of GO (Fig. 1c) corresponds to the d-spacing of 0.83 nm which is similar to the reported values of GO (Shen et al., 2011; Liu et al., 2011). This value is bigger than the d-spacing (0.34 nm) of pristine graphite due to the oxidation and the intercalated water molecules between the layers (Liu et al., 2011). The only one distinct diffraction peak at 10.69º also indicates that synthesized sample is high purity GO.

FTIR spectrum is used to qualitatively examine the nature of surface functionality. As shown in Fig. 1d, GO shows a broad peak at 3420 cm^{-1}, which is related to the OH groups. The peak at 1630 cm^{-1} is due to the skeletal vibrations of unoxidized graphitic domains (Pan et al., 2011). The peaks at 1400 and 1100 cm^{-1} are assigned to asymmetric COOH stretching vibration and alkoxy C-O groups situated at the edges of the GO sheets, respectively (Murugan et al., 2009). The result is similar to the previous report about that for GO synthesized with chemical oxidation method, the oxidation of graphite involves a chemical process to oxidize of carbon atoms at the periphery of the graphite matrix to form oxygen-containing groups including hydroxyl, carboxylic, epoxy or alkoxy groups (Chen et al., 2011).

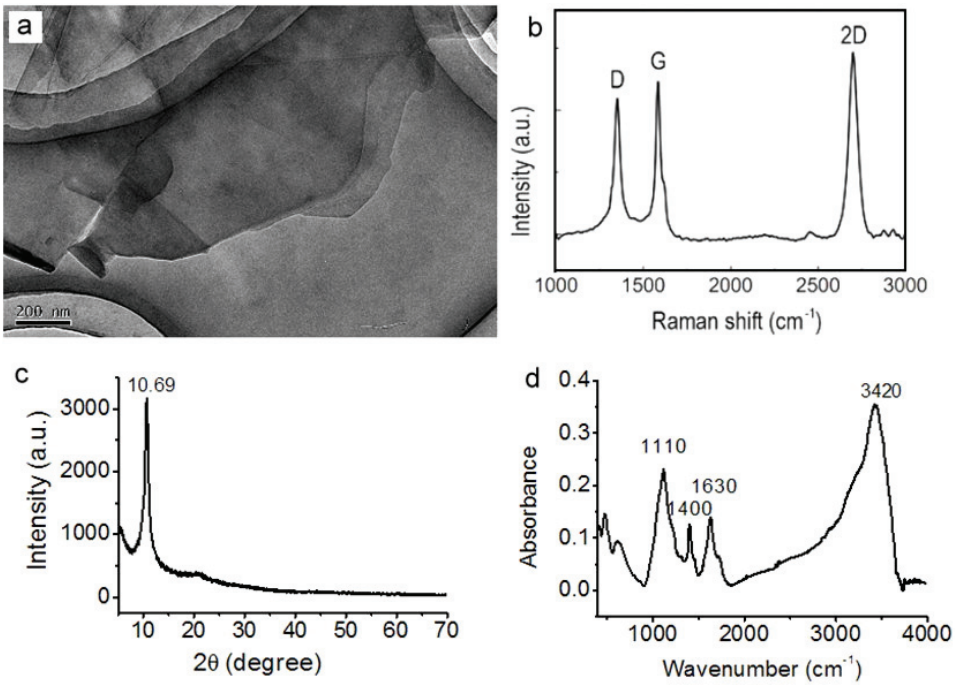

Fig. 1. Characterization of GO: a) TEM image; b) Raman spectrum; c) XRD pattern; d) FTIR spectrum

3.2. Adsorption

3.2.1. Effect of initial pH on adsorption capacity

Adsorption of cationic red X-GRL on the adsorbent was studied at varying pH values. Fig. 2 shows the adsorption capacity and removal percentage of cationic red X-GRL adsorbed by GO. It shows that the initial pH of solution has negligible effect on the cationic red X-GRL adsorption capacity, so the removal process of cationic red X-GRL from the aqueous solution by GO can be carried out at both acidic and basic circumstances.

3.2.2. Effect of adsorbent dosage on removal efficiency

Fig. 3 shows the effect of adsorbent dosage on removal percentage and amount of dye adsorbed by GO at equilibrium. The removal percentage of cationic red X-GRL is more than 94 % at adsorbent dosage is 0.3 g L^{-1}, and it increases up to 99 % by increasing the adsorbent dosage up to 1.3 g L^{-1}. While the adsorption capacity of GO presents declining trend as the dosage increases, the phenomenon may be attributed to the decrease in active sites and agglomeration of the adsorbents.

With the increasing of adsorbent dosage, the active sites of adsorbents provided are greatly more than the saturated threshold adsorption point, so only part of active sites are occupied by cationic red, leading to the decrease of adsorption capacity (Li et al., 2003). In addition, as the adsorbent dosage increase, the diffusion path of dye molecules in GO becomes longer, resulting in the decrease of amount of cationic red X-GRL adsorbed at equilibrium (Unuabonah et al., 2008).

3.2.3. Effect of contact time on removal efficiency

The effect of contact time on cationic red X-GRL adsorbed by GO was studied and shown in Fig. 4. It shows a rapid increase of adsorption capacity in the first 25 min due to the higher driving force making dye molecules transfer to the surface of the adsorbents and the availability of the uncovered active sites (Aroua et al., 2008).

With further increasing time, the diminishing availability of the remaining active sites and the decrease in the driving force make it take long time to reach equilibrium (Wu et al., 2008), so the adsorption rate become slow.

3.2.4. Effect of temperature on adsorption efficiency

The effect of temperature on the adsorption of cationic red X-GRL adsorbed by GO was shown in Fig. 5. The equilibrium adsorption capacity of GO increases from a 160.97 to 227.16 mg g^{-1} at initial dye concentration of 70 mg L^{-1} with increasing temperature from 293 to 333 K, indicating that the adsorption of cationic red X-GRL adsorbed by GO is endothermic reaction.

Increasing temperature can affect the adsorption processes mainly from two aspects. Firstly, it decreases solution viscosity and correspondingly increases the diffusion rate of the adsorbate within the pores of the adsorbents (Boudrahem et al., 2009). Secondly, it can increase the number of the adsorption sites through breaking of some internal bonds near the edge of active surface sites of the adsorbents (Acharya et al., 2009). Thus, rising temperature benefits for the enhancement of the adsorption capacity of dye onto GO.

3.3. Adsorption isotherms

In order to investigate how cationic red X-GRL interact with GO and optimize usage of GO, the Langmuir and the Freundlich isotherms were used to describe adsorption isotherm data obtained at three temperatures (293, 313 and 333 K). The Langmuir isotherm is based on the assumption of adsorption on a homogeneous surface, equivalent sorption energies and no interaction between adsorbed species (Li et al., 2010). The Langmuir equation is expressed as (Eq. 3):

$$q_e = \frac{k_L q_{\max} C_e}{1 + k_L C_e} \quad (3)$$

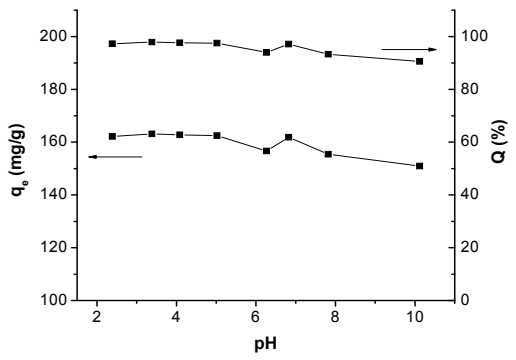

Fig. 2. Effect of pH on cationic red X-GRL adsorbed by GO. Initial dye concentration, 50 mg L^{-1}; GO dosage, 0.3g L^{-1} and temperature, 293K

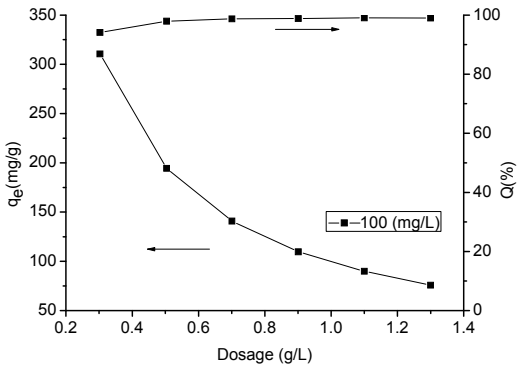

Fig. 3. The effect of adsorbent dose on the adsorption of cationic red X-GRL on GO. Initial concentration, 100 mg L^{-1}; pH 4 and temperature, 293K

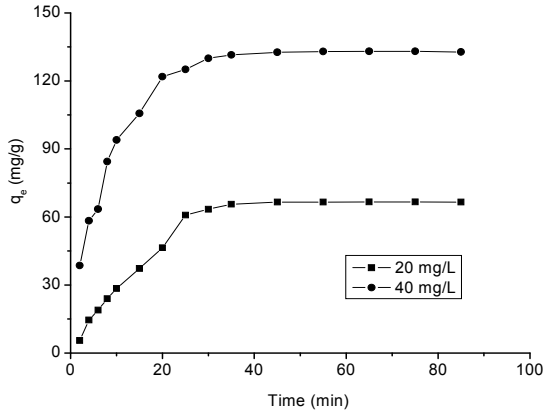

Fig. 4. Effect of contact time on the adsorption of cationic red X-GRL adsorbed by GO. Initial concentration, 40mg L^{-1} and 60 mg L^{-1}; pH 4; GO dosage, 0.3 g L^{-1} and temperature, 293K

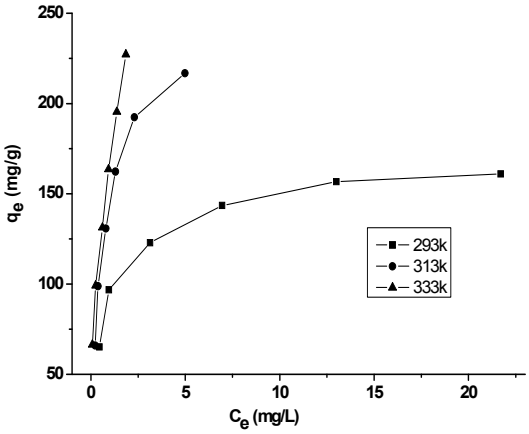

Fig. 5. Effect of temperature on the adsorption of cationic red X-GRL adsorbed by GO. Initial dye concentration, 20-70 mg L^{-1}; pH 4 and GO dosage, 0.3 g L^{-1}

The above equation can be rearranged to the following linear form (Eq. 4):

$$\frac{C_e}{q_e} = \frac{C_e}{q_{\max}} + \frac{1}{q_{\max} k_L} \quad (4)$$

where C_e (mg L^{-1}) is the equilibrium dye concentration, q_{max} (mg g^{-1}) represents the maximum adsorption capacity. k_L (L g^{-1}) is Langmuir constant related to the energy of adsorption, representing the affinity between adsorbent and adsorbate.

Another parameter R_L, a dimensionless equilibrium parameter (Weber and Chakravorti, 1974), which is defined as follows (Eq. 5):

$$R_L = \frac{1}{1 + k_L C_0} \quad (5)$$

where k_L (L g^{-1})is the Langmuir constant and C_0 (mg L^{-1})is the highest initial dye concentration. This value of R_L indicates the type of isotherm to be favorable ($0< R_L <1$), unfavorable ($R_L > 1$), linear ($R_L = 1$), or irreversible ($R_L = 0$) (Ngah et al., 2004).

Freundlich isotherm is an empirical equation based on an exponential distribution of adsorption sites and energies and adsorption process on the non-uniform surface of adsorbents (Li et al., 2010). It is represented as (Eq. 6):

$$ln\, q_e = ln\, k_F + \frac{1}{n} ln\, c_e \quad (6)$$

where k_F (L g^{-1}) and n are the Freundlich constants indicating the adsorption capacity and adsorption intensity. Straight lines were obtained by plotting C_e/q_e against C_e (Fig. 6a) and ln q_e against ln C_e (Fig. 6b). According to the slopes and intercepts, both Langmuir and Freundlich parameters were calculated and listed in Table 1. It can be seen that the experimental data fit the Langmuir equation better than the Freundlich equation from the higher determination coefficients R^2 of the Langmuir than that of the Freundlich at three temperatures. It demonstrates that the adsorption behavior of cationic red X-GRL adsorbed by GO occurs on the homogeneous surface of GO and R_L values between 0 and 1 also indicates that the adsorption of cationic red X-GRL onto GO is favorable. It also shows the maximum adsorption capacity of cationic red X-GRL on GO is 263.16 mg g^{-1} at temperature of 333 K, which is higher than that of graphene (238.10 mg g^{-1}) (Li et al., 2011). The higher adsorption capacity of GO may be due to the π-π stacking interaction between cationic red X-GRL molecules and the surface of GO (Zhao et al., 2011).

3.4. Kinetic studies

To analyze the adsorption kinetics of cationic red X-GRL onto GO, three kinetic models are applied, including pseudo-first-order model, pseudo-second-order, and intra-particle diffusion model.

The pseudo-first-order equation is expressed as follows (Eq. 7):

$$log(q_e - q_t) = log\, q_e - \frac{k_1}{2.303} t \quad (7)$$

where k_1 is the Lagergren rate constant of adsorption (1/min).

The values of q_e and k_1 (Table 2) were determined from the plot of log(q_e-q_t) against t (Fig. 7). The lower determination coefficients R^2 (<0.9374) suggest that adsorption of cationic red X-GRL onto GO does not follow the pseudo-first-order model. The linearized-integral form of the pseudo-second-order model is (Eq. 8):

$$\frac{t}{q_t} = \frac{1}{k_2 q_e^2} + \frac{t}{q_e} \quad (8)$$

where k_2 (g mg^{-1}·min) is the rate constant of pseudo-second-order adsorption.

From the slopes and intercepts of straight portion of the linear plots obtained by plotting t/q_t against t (Fig. 8), the values of k_2 and q_e were calculated and listed in Table 2.

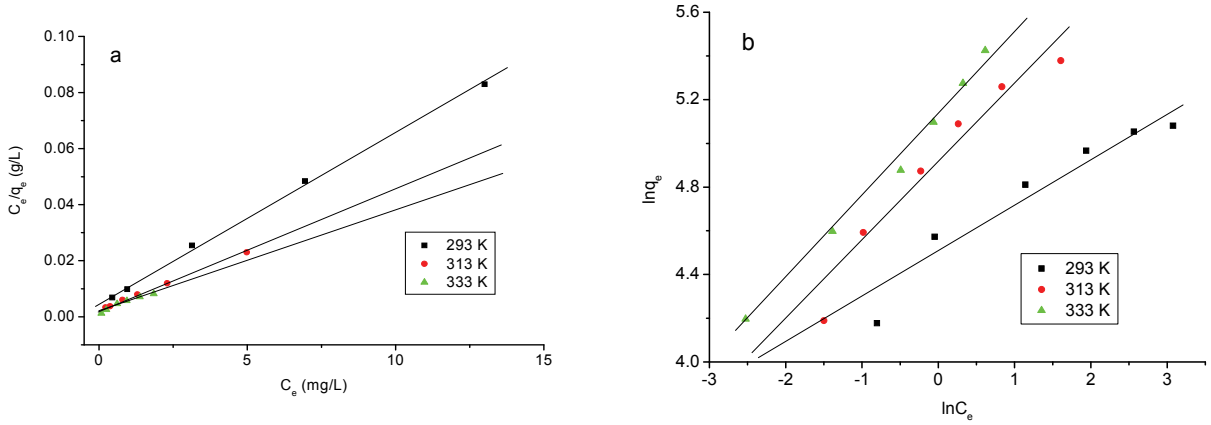

Fig. 6. The equilibrium isotherm for cationic red X-GRL adsorbed by GO: (a) the Langmuir isotherm, (b) the Freundlich isotherm. Initial dye concentration, 20-70 mg L^{-1}; pH 4; and GO dosage, 0.3 g L^{-1}

Table 1. Parameters of Langmuir and Freundlich adsorption isotherm models for X-GRL adsorbed by GO

T (K)	*Langmuir*				*Freundlich*			
	q_{max}(mg g^{-1})	k_L(L g^{-1})	R^2	R_L		n	k_F(L g^{-1})	R^2
293	166.67	1.13	0.9994	0.0125		4.49	88.69	0.9309
313	243.900	1.64	0.9993	0.0086		2.65	133.98	0.9445
333	263.16	2.38	0.9542	0.0060		2.59	170.41	0.9514

The higher determination coefficients (>0.9803) suggests that the pseudo-second-order model is more likely to predict the behavior over the whole experimental range of adsorption. It also means the overall rate of cationic red X-GRL adsorption process seems to be controlled by the chemical process through sharing of electrons or by covalent forces through exchanging of electrons between adsorbent and adsorbate (Malik et al., 2002).

The intra-particle diffusion model is used to predict the rate controlling step (Wang et al., 2010). It can be written as (Eq. 9):

$$q_t = k_i t^{1/2} + C_i \quad (9)$$

where q_t is the amount of cationic red X-GRL adsorbed at time t, k_i (mg g^{-1}·min) is intra-particle diffusion constant at stage i, C_i is the intercept at stage i, and the value of C_i is related to the thickness of the boundary layer. If C_i is not equal to zero, it reveals that the adsorption involves a complex process and the intra-particle diffusion is not the only controlling step for the adsorption (Gerçel et al., 2007). Fig. 9 shows multi-linearity characterizations by plotting q_t vs. $t^{1/2}$. The higher determination coefficients R^2 (>0.9804, Table 2) demonstrate the experimental data fit to the intra-particle diffusion model well. The first sharp stage is the external adsorption stage or instantaneous stage occupying the major part of adsorption process, indicating the external adsorption process is the main controlling stage. The higher slope in the first stage indicates the rate of dye removal is higher, attributing to the instantaneous availability of active adsorption sites. The following is a lower slope, because the decreasing concentration gradient makes the dye molecules take more time into the micropore of GO, leading to a low removal rate. C_I and C_{II} are non-zero, revealing that the adsorption process is rather complex and involves more than one diffusive resistance and controlling stage.

3.5. Thermodynamic studies

The thermodynamic parameters such as the adsorption standard free energy changes (ΔG^0), the standard enthalpy change (ΔH^0) and the standard entropy change (ΔS^0) are obtained from experiments at various temperatures using the following equations (Yao et al., 2010) (Eqs. 10 -12):

$$\Delta G^0 = -RT \ln k_L \quad (10)$$

$$\ln K_L = \Delta S^0 / R - \Delta H^0 / RT \quad (11)$$

$$\Delta G^0 = \Delta H^0 - T\Delta S^0 \quad (12)$$

where R (8.3145 J mol^{-1} K^{-1})is the gas constant, k_L (L g^{-1}) is the Langmuir constant and T (K) is the absolute temperature (Yao et al., 2010).

The values ΔH^0 of and ΔS^0 can be calculated from the slopes and the intercepts of the linear straight by plotting $\ln K_0$ against 1/T. According to the equation (10), the values of ΔG^0 can be calculated. Table 3 shows the values of ΔH^0, ΔS^0 and ΔG^0 at different initial dye concentrations and temperatures. The positive standard enthalpy change (ΔH^0) suggests that the interaction of cationic red X-GRL adsorbed by GO is endothermic, and the positive standard entropy change (ΔS^0) reveals the

increased randomness at the solid-solution interface during the adsorption progress (Nuhoglu et al., 2009). The negative values of ΔG^0 at three temperatures indicates the fact that the adsorption of cationic red X-GRL onto GO is a spontaneous reaction.

The increase in standard free energy changing with the rise in temperature shows an increase in feasibility of adsorption at higher temperature, which verifies the correctness of the experimental results in theory.

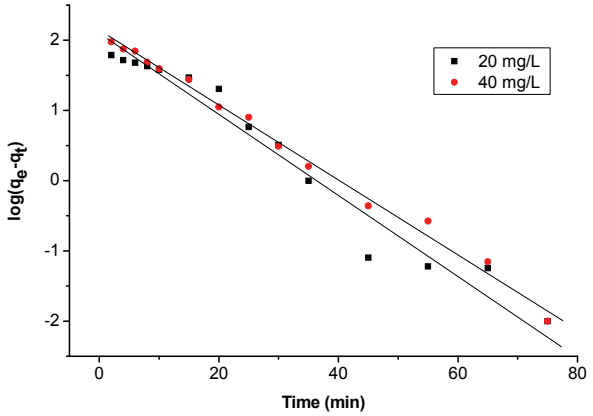

Fig. 7. Pseudo-first order reaction kinetics of cationic red X-GRL adsorbed by GO. Initial concentration, 20 mg L^{-1} and 40 mg L^{-1}; pH 4; GO dosage, 0.3 g L^{-1} and temperature, 293K

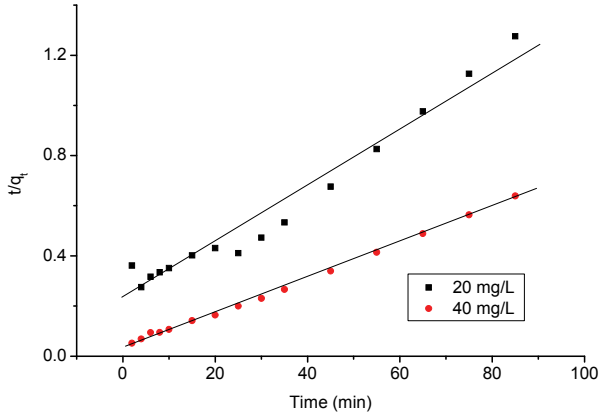

Fig. 8. Pseudo-second order reaction kinetics of cationic red X-GRL adsorbed by GO. Initial concentration, 20 mg L^{-1} and 40 mg L^{-1}; pH 4; GO dosage, 0.3 g L^{-1} and temperature, 293K

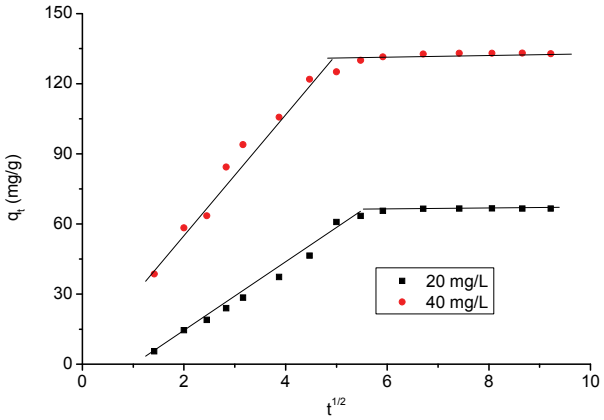

Fig. 9. Intra-particle diffusion of cationic red X-GRL adsorbed by GO. Initial concentration, 20 mg L^{-1} and 40 mg L^{-1}; pH 4; GO dosage, 0.3 g L^{-1} and temperature, 293K

Table 2. Kinetic parameters for cationic red X-GRL adsorbed by GO

Models	***Parameters***	***20 mg L^{-1}***	***40 mg L^{-1}***
Pseudo-first-order	q_e (mg g^{-1})	5.70	5.84
	k_1 (1/min)	0.07	0.06
	R^2	0.9374	0.9262
Pseudo-second-order	q_e (mg g^{-1})	86.8056	143.4720
	K_2 (g $mg^{-1}min^{-1}$) * 10^{-4}	3.0709	143.4720
	R^2	0.9803	0.9977
Intra-particle diffusion	k_I	14.0844	22.9664
	C_I	-15.0354	12.9825
	R^2	0.9913	0.9850
	k_{II}	0.2275	0.3707
	C_{II}	64.6898	129.8410
	R^2	0.9941	0.9804
	q_e (mg g^{-1})	5.7018	5.8447

Table 3. Thermodynamic parameters for cationic red X-GRL adsorbed by GO

Temperature(K)	***ΔG^0 (kJ mol^{-1})***	***ΔH^0(kJ mol^{-1})***	***ΔS^0(J $k^{-1}mol^{-1}$)***
293	-0.2799	15.085	52.44
313	-1.3287		
333	-2.3775		

4. Conclusion

GO was prepared from expandable graphite by a modified Hummers' method and characterized by TEM, XRD, FTIR, and Raman spectroscopy. Batch adsorption experiments show that the initial pH of solution has negligible effect on the cationic red X-GRL adsorption capacity. The adsorption kinetic was best in accordance with the pseudo-second-order model. The Langmuir isotherm was better to fit the experimental data compared with the Freundlich model. The monolayer adsorption capacities of GO are 166.67 and 263.16 mg g^{-1} at temperatures of 293 and 333 K, respectively, suggesting that GO, as a new kind of adsorbent, may have great potential application in dye removal from aqueous solutions.

Acknowledgements

This work was supported by Natural Science Foundation of Qingdao (12-1-4-2-（23）-jch), the National Natural Science Foundation of China (50802045 and 20975056), Natural Science, Program of NSFC-JSPS (21111140014), the Taishan Scholar Program of Shandong Province, and Program for Changjiang Scholars and Innovative Research Team in University (IRT0970), National Key Basic Research Development Program of China (973 special preliminary study plan) (Grant no.: 2012CB722705).

References

Acharya J., Sahu J.N., Mohanty C.R., Meikap B.C., (2009), Removal of lead(II) from wastewater by activated carbon developed from Tamarind wood by zinc chloride activation, *Chemical Engineering Journal,* **149**, 249–262.

Alpat S.K., Özbayrak Ö., Alpat Ş., Akçay H., (2008), The adsorption kinetics and removal of cationic dye, Toluidine Blue O, from aqueous solution with Turkish zeolite, *Journal of Hazardous Materials* **151**, 213–220.

Aroua M.K., Leong S.P.P., Teo L.Y., Yin C.Y., Daud W.M.A.W., (2008), Real-time determination of kinetics of adsorption of lead(II) onto palm shell-based activated carbon using ion selective electrode, *Bioresource Technology*, **99** , 5786–5792.

Balandin A.A., Ghosh S., Bao W.Z., Calizo I., Teweldebrhan D., Miao F., Lau C.N., (2008), Superior thermal conductivity of single-layer graphene, *Nano Letters*, **8**, 902–907.

Boudrahem F., Aissani-Benissad F., Aït-Amar H., (2009), Batch sorption dynamics and equilibrium for the removal of lead ions from aqueous phase using activated carbon developed from coffee residue activated with zinc chloride, *Journal of Environment Management*, **90**, 3031–3039.

Calizoa I., Ghosh S., Bao W., Miao F., Lau C.N., Balandin A.A., (2009), Raman nanometrology of graphene: temperature and substrate effects, *Solid State Communications,* **149**, 1132–1135.

Chen G., Zhai S., Zhai Y., Zhang K., Yue Q., Wang L., Zhao J., Wang H., Liu J., Jia J., (2011), Preparation of sulfonic-functionalized graphene oxide as ion-exchange material and its application into electrochemiluminescence analysis, *Biosensors and Bioelectronics,* **26**, 3136–3141.

Ciardelli G., Corsi L., Marucci M., (2000), Membrane separation for wastewater reuse in the textile industry, *Resource Conservation and Recycling,* **31**, 189–197.

Cuong T.V., Pham V.H., Tran Q.T., Chung J.S., Shin E.W., Kim J.S., Kim E.J., (2010), Optoelectronic properties of graphene thin films prepared by thermal reduction of graphene oxide, *Materials Letters,* **64**, 765–767.

Gerçel Ö., Gerçel H.F., (2007), Adsorption of lead(II) ions from aqueous solutions by activated carbon prepared from biomass plant material of Euphorbia rigida, *Chemical Engineering Journal*, **132**, 289–297.

Harja M., Barbuta M., Rusu L., Munteanu C., Buema G., Doniga E., (2011), Simultaneous removal of astrazone blue and lead onto low cost adsorbents based on power plant ash, *Environmental Engineering and Management Journal*, **10**, 341-347.

Hummers W.S., Offeman R.E., (1958), Preparation of graphitic oxide, *Journal of the American Chemical Society,* **80**, 1339.

Koch M., Yediler A., Lienert D., Insel G., Kettrup A., (2002), Ozonation of hydrolyzed azo dye reactive yellow 84 (CI), *Chemosphere*, **46**, 109–113.

Lee C.G., Wei X.D., Kysar J.W., Hone J., (2008), Measurement of the elastic properties and intrinsic strength of monolayer graphene, *Science*, **321**, 385–388.

Li Y.H., Luan Z., Xiao X., Zhou X., Xu C., Wu D., Wei B., (2003), Removal of Cu^{2+} ions from aqueous solutions by carbon nanotubes, *Adsorption Science and Technology,* **21**, 475-485.

Li Y.H., Du Q., Wang X., Zhang P., Wang D., Wang Z., Xia Y., (2010), Removal of lead from aqueous solution by activated carbon prepared from Enteromorpha prolifera by zinc chloride activation, *Journal of Hazardous Materials,* **183**, 583–589.

Li Y.H., Liu T., Du Q., Sun J., Xia Y., Wang Z., Zhang W., Wang K., Zhu H., Wu D., (2011), Adsorption of cationic red X-GRL from aqueous solutions by graphene: equilibrium, kinetics and thermodynamics study,*Chemical and Biochemical Engineering Quarterly*, **25**, 483–491.

Liu Y., Liu C.Y., Liu Y.Y., (2011), Investigation on fluorescence quenching of dyes by graphite oxide and graphene, *Applied Surface Science*, **257**, 5513–5518.

Liu T.H., L Y., Du Q., Sun J., Jiao Y., Yang G., Wang Z., Xia Y., Zhang W., Wang K., Zhu H., Wu D., (2012), Adsorption of methylene blue from aqueous solutions by graphene, *Colloids and Surfaces B: Biointerfaces*, **90**,197-203.

Malik D.J., Strelko Jr. V., Streat M., Puziy A.M., (2002), Characterisation of novel modified active carbons and marine algal biomass for the selective adsorption of lead, *Water Research,* **36**, 1527–1538.

Malik P.K., Saha S.K., (2003), Oxidation of direct dyes with hydrogen peroxide using ferrous ion as catalyst, *Separation and Purification Technology*, **31**, 241–250.

Morozov S.V., Novoselov K.S., Shedin F., Jiang D., Firsov A.A., Geim A.K., (2005), Two-dimensional electron and hole gases at the surface of graphite, *Physical Review B,* **72**, 201401-1-4.

Murugan A.V., Muraliganth T., Manthiram A., (2009), Rapid, facile microwave solvothermal synthesis of graphene nanosheets and their polyaniline nanocomposites for energy storage, *Chemistry of Materials,* **21**, 5004-5006.

Ngah W.S.W., Kamari A., Koay Y.J., (2004), Equilibrium and kinetics studies of adsorption of copper(II) on chitosan and chitosan/PVA beads, *International Journal of Biological Macromolecules*, **34**, 155-161.

Nuhoglu Y., Malkoc E., (2009), Thermodynamic and kinetic studies for environmentaly friendly Ni(II) biosorption using waste pomace of olive oil factory, *Bioresource Technology,* **100**, 2375–2380.

Pan Y., Wu T., Bao H., Li L., (2011), Green fabrication of chitosan films reinforced with parallel aligned graphene oxide, *Carbohydrate Polymers*, **83**, 1908–1915.

Panswed J., Wongchaisuwan S., (1986), Mechanism of dye wastewater color removal by magnesium carbonate-hydrated basic, *Water Science and Technology,* **18**, 139–144.

Park S., Ruoff R.S., (2009), Chemical methods for the production of graphenes, *Nature Nanotechnology,* **4**, 17–224.

Purkait M.K., DasGupta S., De S., (2003), Removal of dye from wastewater using micellar enhanced ultrafiltration and recovery of surfactant, *Separation and Purification Technology,* **37**, 81–92.

Rao C.N.R., Biswas K., Subrahmanyam K.S., Govindaraj A., (2009), Graphene, the new nanocarbon, *Journal of Materials Chemistry*, **19**, 2457–2469.

Robinson T., McMullan G., Marchant R., Nigam P., (2001), Remediation of dyes in textile effluent: a critical review on current treatment technologies with a proposed alternative, *Bioresource Technology*, **77**, 247-255.

SenthilKumar P., Umaiyambika N., Gayathri R., (2010), Dye removal from aqueous solution by electrocoagulation process using stainless steel electrodes, *Environmental Engineering and Management Journal*, **9**, 1031-1037.

Shen J., Hu Y., Shi M., Lu X., Qin C., Li C., Ye M., (2009), Fast and facile preparation of graphene oxide and reduced graphene oxide nanoplatelets, *Chemistry of Materials*, **21**, 3514–3520.

Shen J., Shi M., Yan B., Ma H., Li N., Ye M., (2011), One-pot hydrothermal synthesis of Ag-reduced graphene oxide composite with ionic liquid, *Journal of Materials Chemistry*, **21**, 7795–7801.

Sreeprasad T.S., Maliyekkal S.M., Lisha K.P., Pradeep T., (2011), Reduced graphene oxide–metal/metal oxide composites: Facile synthesis and application in water purification, *Journal of Hazardous Materials*, **186**, 921–931.

Sun Q., Yang L., (2003), The adsorption of basic dyes from aqueous solution on modified peat–resin particle, *Water Research,* **37**, 1535–1544.

Unuabonah E.I., Adebowale K.O., Olu-Owolabi B.I., Yang L.Z., Kong L.X., (2008), Adsorption of Pb(II) and Cd(II) from aqueous solutions onto sodium tetraborate modified kaolinite clay: equilibrium and thermodynamic studies, *Hydrometallurgy*, **63**, 1-9.

Wang L., Zhang J., Zhao R., Li Y., Li C., Zhang C., (2010), Adsorption of Pb(II) on activated carbon prepared from polygonum orientale Linn.: kinetics, isotherms, pH, and ionic strength studies, *Bioresource Technology*, **101**, 5808–5814.

Weber W.J., Chakravorti R.K., (1974), Pore and solid diffusion models for fixed bed adsorbers, *American Institute of Chemical Engineers*, **20,** 228–238.

Wu Y., Zhang S., Guo X., Huang H., (2008), Adsorption of chromium(III) on lignin, *Bioresource Technology*, **99**, 7709–7715.

Yang S.T., Chang Y., Wang H., Liu G., Chen S., Wang Y., Liu Y., Cao A., (2010), Folding/aggregation of graphene oxide and its application in Cu^{2+} removal, *Journal of Colloid and Interface Science*, **351**, 122-127.

Yang S.T., Chen S., Chang Y., Cao A., Liu Y., Wang H., (2011), Removal of methylene blue from aqueous solution by graphene oxide, *Journal of Colloid and Interface Science*, **359**, 24-29.

Yao Y.J., Xu F.F., Chen M., Xu Z.X., Zhu Z.W., (2010), Adsorption behavior of methylene blue on carbon nanotubes, *Bioresource Technology*, **101**, 3040-3046.

Zhang K., Dwivedi V., Chi C., Wu J., (2010a), Graphene oxide/ferric hydroxide composites for efficient arsenate removal from drinking water, *Journal of Hazardous Materials*, **182**, 162–168.

Zhang W.L., Park B.J., Choi H.J., (2010b), Colloidal graphene oxide/polyaniline nanocomposite and its electrorheology, *Chemical Communications,* **46**, 5596–5598.

Zhao G., Li J., Wang X., (2011), Kinetic and thermodynamic study of 1-naphthol adsorption from aqueous solution to sulfonated graphene nanosheets, *Chemical Engineering Journal*, **173**, 185-190.